SLAC-PUB-10151
August 2003
hep-ph/0308101

RADIATIVE PENGUIN DECAYS FROM *BABAR*

G. Eigen

Representing the BABAR Collaboration

Invited talk presented at the 2nd Workshop on the CKM Unitarity Triangle,
4/5/2003—4/9/2003, Durham, England

Stanford Linear Accelerator Center, Stanford University, Stanford, CA 94309

Work supported by Department of Energy contract DE–AC03–76SF00515.

Workshop on the CKM Unitarity Triangle, IPPP Durham, April 2003

Radiative Penguin Decays from *BABAR*

G Eigen (representing the *BABAR* collaboration)

Department of Physics, University of Bergen

We summarize the latest *BABAR* results on $B \to K^{(*)}\ell^+\ell^-$ and $B \to \rho(\omega)\gamma$.

1 Introduction

Electroweak penguin decays provide a promising hunting ground for Physics beyond the Standard Model (SM). The decay $B \to X_s\gamma$, which proceeds through an electromagnetic penguin loop, already provides stringent constraints on the supersymmetric (SUSY) parameter space [1]. The present data samples of $\sim 1 \times 10^8 B\overline{B}$ events allow to explore radiative penguin decays with branching fractions of the order of 10^{-6} or less. In this brief report we discuss a study of $B \to K^{(*)}\ell^+\ell^-$ decay modes and a search for $B \to \rho(\omega)\gamma$ decays.

2 Study of $B \to K\ell^+\ell^-$ and $B \to K^*\ell^+\ell^-$

The decays $B \to K\ell^+\ell^-$ and $B \to K^*\ell^+\ell^-$ proceed through an electromagnetic penguin loop, a Z^0 penguin loop or a weak box diagram as shown in Figure 1. In the framework of the operator product expansion (OPE) the decay rate is factorized into perturbatively calculable short-distance contributions that are parameterized by scale-dependent Wilson coefficients and non-perturbative long-distance effects that are represented by local four-quark operators. Operator mixing occurring in next-to-leading order perturbation theory leads to three effective scale-dependent (μ_b) Wilson coefficients, $C_7^{eff}(\mu_b), C_9^{eff}(\mu_b)$, and $C_{10}^{eff}(\mu_b)$ that are each sensitive to New Physics contributions. Examples for non-SM penguin loops are depicted in Figure 2. In the Standard Model the branching fractions are predicted to be within the following ranges, $\mathcal{B}(B \to K\ell^+\ell^-) = (0.23-0.97)\times10^{-6}$, $\mathcal{B}(B \to K^*\mu^+\mu^-) = (0.81-2.64)\times10^{-6}$ and $\mathcal{B}(B \to K^*e^+e^-) = (1.09-3.0)\times10^{-6}$ [2]. In supersymmetric models, for example, the branching fractions my be enhanced by more than a factor of two [1].

BABAR has analyzed eight final states where a $K^\pm, K_S^0, K^{*0}$ or $K^{*\pm}$ recoils against a $\mu^+\mu^-$ or e^+e^- pair, using an integrated luminosity of 77.8 fb^{-1} that corresponds to $(84.4 \pm 0.9) \times 10^6$ $B\overline{B}$ events. The discriminating variables are beam energy-substituted mass $m_{ES} = \sqrt{(E^*_{beam})^2 - (\vec{p}^*_B)^2}$ and the energy difference $\Delta E^* = E^*_B - E^*_{beam}$, where $\vec{p}_B$, E^*_B and E^*_{beam} denote the B-momentum, B-energy and beam energy in the center-of-mass (CM) frame, respectively. The $\Delta E^* - m_{ES}$ *plane* is divided into three regions, a signal region ($\pm3\sigma$ boxes around the signal), the fit region ($m_{ES} > 5.2$ GeV, $|\Delta E^*| < 250$ MeV), and a large side band ($m_{ES} > 5.0$ GeV, $|\Delta E^*| < 500$ MeV). Specific selection criteria are used to suppress individual backgrounds. A Fisher discriminant [5] is used to eliminate the back-to-back continuum background. It is based on event shape variables such as the thrust angle between the daughter particles of the B meson candidate and that of the remaining particles in the event ($\cos\theta_T$), the B decay angle in the $\Upsilon(4S)$ rest frame between the B candidate and the beam axis ($\cos\theta^*_B$), and the ratio of second-to-zeroth Fox-Wolfram moments (R_2) [3], as well as the invariant mass of the $K-\ell$ system $m_{k\ell}$. To discriminate against combinatorial $B\overline{B}$ background a likelihood function is used that combines the missing energy in the event (E_{miss}), with the dilepton vertex probability, the significance of the dilepton separation along the beam direction and $\cos\theta^*_B$. To reject events from $B \to J/\psi K^{(*)}$ and $B \to \psi(2S)K^{(*)}$ decays with $J/\psi(\psi(2S) \to \ell^+\ell^-$ that have the same event topologies in a restricted $m_{\ell\ell}$ mass region as signal events, the shaded regions in the $\Delta E^* - m_{\ell\ell}$ plane shown in Figure 3 are vetoed. The inclined bands provide an efficient rejection of $J/\psi K^{(*)}$ events in the fit region, in which one or both leptons radiated a photon.

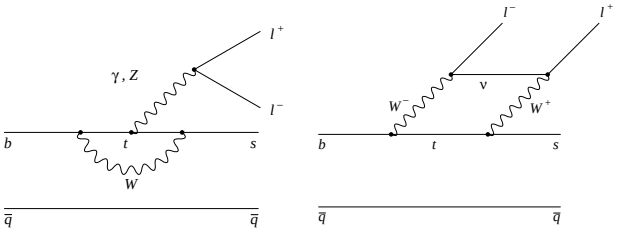

Figure 1. Lowest-order diagrams for $B \to K^{(*)}\ell^+\ell^-$ in SM.

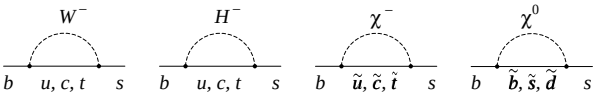

Figure 2. Penguin loop diagrams involving a W boson, a charged Higgs boson, a chargino and a neutralino, respectively.

The selection criteria are optimized on simulated data as

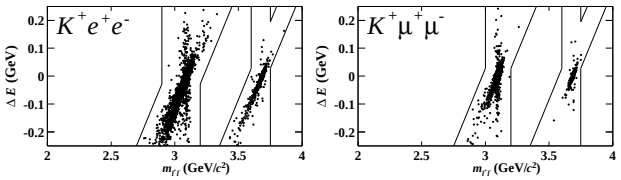

Figure 3. Charmonium veto (hatched regions) in the $\Delta E^* - m_{\ell^+\ell^-}$ plane for $B \to K^{(*)}e^+e^-$ and $B \to K^{(*)}\mu^+\mu^-$. The dots represent simulations for $B \to J/\psi(\to \ell^+\ell^-)K^{(*)}$ and $B \to \psi(2S)(\to \ell^+\ell^-)K^{(*)}$.

well as data sidebands. The simulated data are used to determine efficiencies and estimate the contribution of backgrounds that may peak in the $\Delta E^* - m_{ES}$ signal box. Specifically, the decay channels $B \to K^*\gamma$, $B \to J/\psi K^{(*)}$, $B \to \psi(2S)K^{(*)}$, $B \to K^{(*)}\pi^0$, $B \to K^{(*)}\eta$, $B \to K\pi\pi$, $B \to KK\pi$, $B \to KKK$, and $B \to D\pi$ have been studied. The Monte Carlo results are checked with data control samples, including exclusive and inclusive charmonium decays, $B \to D\pi$ decays, data sidebands and $K^{(*)}e^\pm\mu^\mp$ samples. For the combined exclusive charmonium modes we achieve an excellent agreement between data and Monte Carlo for the ratio of event yields of 1.013 ± 0.018. Further details of the event selection are discussed in [6].

In each of the four $K\ell^+\ell^-$ final states, a signal is extracted from a two-dimensional fit to the $m_{ES} - \Delta E^*$ plane. Similarly, a signal yield for the four $K^*\ell^+\ell^-$ final states is obtained from a three-dimensional fit to the $m_{ES} - \Delta E^* - m_{k\pi}$ space. The signal shapes are obtained from Monte Carlo samples with fine-tuning on the exclusive charmonium modes. To account for the asymmetric ΔE^* and M_{ES} distributions that result from radiation effects of the final-state leptons and correlations in the two variables a product of Crystal Ball functions is used [7]. The combinatorial backgrounds are parameterized with ARGUS functions [8], where both the normalization and the shape parameters are left free. Only in $B \to K^\pm e^+e^-$, a significant yield of $16.2^{+4.8}_{-4.1}$ events is observed. The selection efficiency is $(19.1 \pm 1.1)\%$, yielding a branching fraction of

$$\mathcal{B}(B^+ \to K^+e^+e^-) = (0.96^{+0.28}_{-0.24} \pm 0.06) \times 10^{-6} \qquad (1)$$

The second largest yield of $(7.8^{+5.4}_{-4.2})$ events is found for $B^0 \to K^{*0}e^+e^-$ for which a selection efficiency of $(10.6 \pm 0.9)\%$ is achieved. The individual results for each of the eight final states are summarized in Table 1.

The M_{ES} and ΔE^* projections of the two-dimensional fit for the combined $B \to K\ell^+\ell^-$ final states are shown in Figure 4. The corresponding distributions of the three-dimensional fit for the combined $B \to K^*\ell^+\ell^-$ channels as well as the $m_{K\pi}$ mass projection are shown in Figure 5. In order to combine $K^*\mu^+\mu^-$ and $K^*e^+e^-$ results their ratio of branching fractions is assumed to be $\mathcal{B}(B \to K^*e^+e^-)/\mathcal{B}(B \to K^*\mu^+\mu^-) = 1.33$ [1]. The multiplicative systematic errors that do not affect the significance

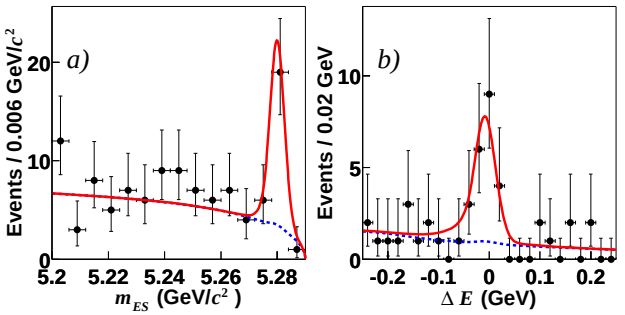

Figure 4. Projections of the two-dimensional fit of the combined $K\ell^+\ell^-$ data sample for a) m_{ES} after the constraint $-0.11 < \Delta E^* < 0.05$ GeV and b) ΔE^* after requiring $|m_{ES} - m_B| < 6.6$ MeV/c^2. The solid and dashed curves show the entire fit and the total background contribution, respectively.

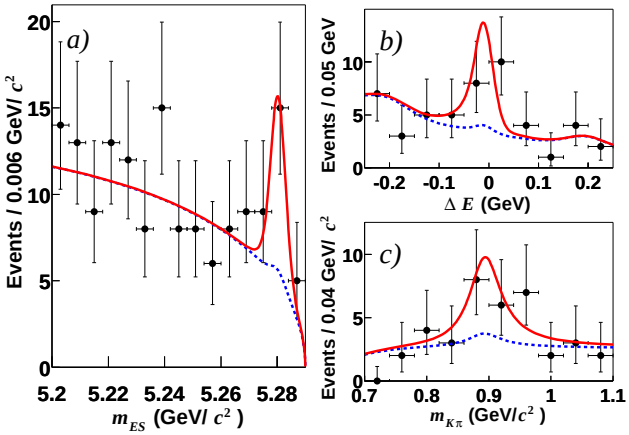

Figure 5. Projections of the tree-dimensional fit of the combined $K^*\ell^+\ell^-$ data sample for a) m_{ES} after the constraint $-0.11 < \Delta E^* < 0.05$ GeV and $0.817 < m_{K\pi} < 0.967$ *MeV*, b) ΔE^* after requiring $|m_{ES} - m_B| < 6.6$ MeV/c^2 and $0.817 < m_{K\pi} < 0.967$ *MeV*, and c) $m_{K\pi}$ satisfying $-0.11 < \Delta E^* < 0.05$ GeV and $|m_{ES} - m_B| < 6.6$ MeV/c^2. The solid and dashed curves show the entire fit and the total background contribution, respectively.

range from 6% – 12% for $K\ell^+\ell^-$ modes and 7% – 15% for $K^*\ell^+\ell^-$ modes. The largest contributions result from the K^0_S efficiency (10%), the model dependence (4% – 7%), μ identification (3.2%), $B\bar{B}$ likelihood ratio (1.3% – 5.6%), the Fisher discriminant (0.9% – 3.1%), and the tracking efficiency for hadrons (1.3% – 3.9%). Contributions from K/π identification, e identification, tracking efficiency for leptons, Monte Carlo statistics and $B\bar{B}$ counting are small (1% – 2%). The additive systematic errors that affect the significance result from the signal yields in the fit, including uncertainties in signal shapes, background shapes and the amount of peaking backgrounds. Including systematic errors the significance of the combined $K\ell^+\ell^-$ sample is 7.0σ, while that of the combined $K^*\ell^+\ell^-$ sample is 3.0σ.

For the combined $B \to K\ell^+\ell^-$ modes we measure a

Table 1. Measured event yields, efficiencies and branching fractions for $B \to K\ell^+\ell^-$ and $B \to K^*\ell^+\ell^-$ modes.

Mode	yield [events]	ϵ[%]	$\mathcal{B} \times 10^6$
$B^+ \to K^+e^+e^-$	$16.2^{+4.8}_{-4.1}$	19.1 ± 1.1	$0.96^{+0.28+0.06}_{-0.24-0.06}$
$B^+ \to K^+\mu^+\mu^-$	$1.0^{+2.0}_{-1.2}$	8.7 ± 0.6	$0.14^{+0.25+0.02}_{-0.16-0.02}$
$B^0 \to K^0e^+e^-$	$-0.5^{+1.6}_{-1.0}$	20.6 ± 2.5	$-0.08^{+0.25+0.05}_{-0.16-0.05}$
$B^0 \to K^0\mu^+\mu^-$	$5.0^{+2.8}_{-2.0}$	9.2 ± 0.7	$1.78^{+0.99+0.22}_{-0.73-0.22}$
$B^0 \to K^{*0}e^+e^-$	$7.8^{+5.4}_{-4.2}$	13.5 ± 0.9	$0.98^{+0.68+0.18}_{-0.54-0.18}$
$B^0 \to K^{*0}\mu^+\mu^-$	$4.5^{+3.8}_{-2.8}$	6.5 ± 0.6	$1.18^{+0.99+0.26}_{-0.73-0.26}$
$B^+ \to K^{*+}e^+e^-$	$2.7^{+4.1}_{-2.9}$	10.2 ± 1.4	$1.31^{+1.97+0.33}_{-1.38-0.33}$
$B^+ \to K^{*+}\mu^+\mu^-$	$4.4^{+3.5}_{-2.4}$	5.0 ± 0.8	$4.33^{+3.41+0.68}_{-2.40-0.68}$

branching fraction of

$$\mathcal{B}(B \to Ke^+e^-) = (0.68^{+0.17}_{-0.15} \pm 0.04) \times 10^{-6}. \quad (2)$$

For the combined $B \to K^*\ell^+\ell^-$ modes we determine a branching fraction of

$$\mathcal{B}(B^+ \to K^*e^+e^-) = (1.4^{+0.57}_{-0.49} \pm 0.21 \times 10^{-6}. \quad (3)$$

The *BABAR* results are consistent with those obtained by BELLE [9] and most SM predictions, but $\mathcal{B}(B \to K\ell^+\ell^-)$ is almost 2σ higher than a recent next-to-next-to-leading order prediction of $\mathcal{B}(B^+ \to K\ell^+\ell^-) = (0.35 \pm 0.12) \times 10^{-6}$ [1].

3 Search for $B \to \rho(\omega)\gamma$

The decays $B \to \rho(\omega)\gamma$ are flavor-changing neutral current $b \to d$ transitions that are mediated by an electromagnetic penguin loop. The decay rates depend on the effective Wilson coefficient $C_7^{eff}(\mu_b)$ that may be enhanced by New Physics contributions as in $B \to K^*\gamma$. They are, however, suppressed with respect to $B \to K^*\gamma$ by $|V_{td}/V_{ts}|^2$. Thus, measuring the ratio of branching fractions $\mathcal{B}(B \to \rho\gamma)/\mathcal{B}(B \to K^*\gamma)$, allows us to extract $|V_{td}/V_{ts}|$. In SM the branching fraction for the charged mode in next-to-leading order is predicted to lie between $\mathcal{B}(B^+ \to \rho^+\gamma) = (0.85 \pm 0.4) \times 10^{-6}$ [12] and $\mathcal{B}(B \to \rho^+\gamma) = (1.58^{+0.53}_{-0.46}) \times 10^{-6}$ [13]. For the neutral modes the branching fractions are a factor of two smaller than that for $B^+ \to \rho^+\gamma$ due to isospin. By determining the ratio of decay rates $\Gamma(B \to \rho\gamma)/\Gamma(B \to K^*\gamma)$ uncertainties due to scale dependence and a precise knowledge of form factors cancel except for SU(3) breaking effects. The largest remaining theoretical uncertainties result from contributions of *W*-annihilation/W-exchange diagrams, which amount to $\sim 20\%$ in $B^+ \to \rho^+\gamma$ and to $\sim 13\%$ in $B^0 \to \rho^0(\omega)\gamma$ [12].

BABAR has searched for $B \to \rho(\omega)\gamma$ modes using an integrated luminosity of 77.8 fb^{-1} on the $\Upsilon(4S)$ peak and 9.6 fb^{-1} in the continuum 40 MeV below the $\Upsilon(4S)$ peak. Challenges in the analysis stem from a huge $q\bar{q}$ continuum background including initial-state radiation, background from $B \to K^*\gamma$ and the fact that the ρ resonance is much broader than the K^* resonance. The $q\bar{q}\gamma$ continuum background with a hard γ from initial-state radiation may have a similar event shape as that of the signal which is less spherical than a typical $B\bar{B}$ event. Photon candidates with energies of 1.5 GeV $< E_\gamma <$ 3.5 GeV that are inconsistent with originating from a π^0 or η decay are combined with a ρ^+, ρ^0, or ω candidate, where the vector mesons are reconstructed from $\pi^+\pi^0$, $\pi^+\pi^-$ and three-pion combinations, respectively. Rejecting charged tracks in the signal that are consistent with a kaon, the K/π misidentification is less than 1%. The $\pi\pi$ (3π) invariant mass has to lie within a mass window of 520 – 1020 MeV/c^2 (759.6 – 805.6 MeV/c^2) and its momentum in the CM frame must satisfy $2.3 < p^*_{\pi\pi} < 2.85$ GeV/c ($2.4 < p^*_{3\pi} < 2.8$ GeV/c). A π^0 candidate must have a $\gamma\gamma$ invariant mass of $115 < m_{\gamma\gamma} < 150$ MeV/c^2. To improve the momentum resolution we perform a kinematic fit with $m_{\gamma\gamma}$ constrained to the nominal π^0 mass.

To reduce the $q\bar{q}$ continuum background a neural network is used that is based on event-shape variables ($\cos\theta_{thrust}, \cos\theta^*_B, \cos\theta_{helicity}$), the Dalitz decay angle for ω, the energy flow in 18 cones around photon direction, the vertex separation Δz, the ratio of second-to-zeroth Fox Wolfram moment, R_2', calculated in a frame recoiling the photon and the net flavor in the event [10]. The neural network is trained with Monte Carlo signal events and continuum data. The neural network output is cross-checked with data using a $B^0 \to D^-\pi^+$ sample that has a similar topology as the signal and the off-resonance data sample. Further details of the event selection are discussed in [11].

The $\Delta E^* - m_{ES}$ distributions for the final data samples are shown in Figure 6. The signal yields are extracted from a maximum likelihood fit in the three-dimensional space $\Delta E^* - m_{ES} - m_\rho(m_\omega)$. The procedure is crosschecked with our $B \to K^*\gamma$ data samples. For $B \to K^{*0}$ (K^{*+})γ the maximum likelihood fit yields 343.2 ± 21.0 (93.1 ± 12.6) events, which is in good agreement with the expected yields of 332 ± 36 (105 ± 18) events, respectively.

The extracted signal yields of $4.8^{+5.2}_{-4.7}$ events for $B \to \rho^0\gamma$, $6.2^{+7.2}_{-6.2}$ events for $B \to \rho^+\gamma$, and $0.1^{+2.7}_{-2.0}$ events for $B \to \omega\gamma$ are consistent with background. The efficiencies are 12.3%, 9.2% and 4.6%, respectively. Including systematic errors, which respectively increase from 11.8% to 13.4% and 17.3% for the three decay channels, we obtain branching fraction upper limits @ 90% *CL* of $\mathcal{B}(B^0 \to \rho^0\gamma) < 1.2 \times 10^{-6}$,
$\mathcal{B}(B^+ \to \rho^+\gamma) < 2.1 \times 10^{-6}$, and $\mathcal{B}(B^0 \to \omega\gamma) < 1.0 \times 10^{-6}$. These limits are significantly lower than those of previous searches [16][17].

Assuming isospin symmetry the $\rho^+\gamma$ and $\rho^0\gamma$ samples are

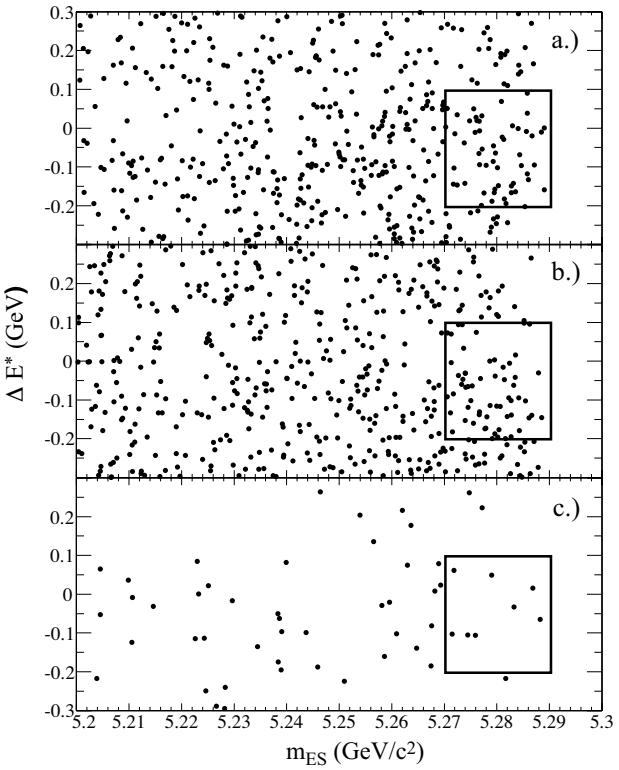

Figure 6. $\Delta E^* - m_{ES}$ scatter plots of the fit region for a) $B^+ \to \rho^+\gamma$, b) $B^0 \to \rho^0\gamma$ and c) $B^0 \to \omega\gamma$ candidates. The boxes indicate the expected signal regions

combined yielding $\mathcal{B}(B \to \rho\gamma) < 1.9 \times 10^{-6}$. Using the recent *BABAR* $B \to K^*\gamma$ branching fraction measurement [14] this translates into an upper limit on the ratio of branching fractions of $\mathcal{B}(B \to \rho\gamma)/\mathcal{B}(B \to K^*\gamma) < 0.047$ @ 90% *CL*. To constrain the ratio of $|V_{td}/V_{ts}|$ we use the parameterization [12].

$$\frac{\mathcal{B}(B \to \rho\gamma)}{\mathcal{B}(B \to K^*\gamma)}) = \left|\frac{V_{td}}{V_{ts}}\right|^2 \left(\frac{1 - m_\rho^2/M_B^2}{1 - m_{K^*}^2/M_B^2}\right)^3 \zeta^2[1 + \Delta R]. \qquad (4)$$

The parameter ζ represents $SU(3)$ breaking while ΔR accounts for the annihilation diagram in $B^+ \to \rho^+\gamma$. Using $\zeta = 0.76 \pm 0.1$ and $\Delta R = 0.0 \pm 0.2$ ([12], [15]) we obtain an upper limit of $|V_{td}/V_{ts}| < 0.34$ @ 90% *CL*. This is still larger than the limit of $|V_{td}/V_{ts}| < 0.23$ @ 95% *CL* which is derived from $B_s\bar{B}_s$ and $B_d\bar{B}_d$ mixing results for $\Delta m_{B_d} = 0.503 \pm 0.006$ ps^{-1}, $\Delta m_{B_s} > 14.4$ ps^{-1} @ 95% CL and $\xi = 1.24$ [18].

The present upper limits are approaching the theoretical predictions. Assuming a branching fraction of $\mathcal{B}(B^+ \to \rho^+\gamma) = 1 \times 10^{-6}$ and $\mathcal{B}(B^0 \to \rho^0\gamma = \mathcal{B}(B \to \omega\gamma = \frac{1}{2}\mathcal{B}(B^+ \to \rho^+\gamma)$ we estimate a signal significance and experimental errors for different luminosities as listed in Table 2. The small values for the significance (*i.e.* large experimental errors on the branching fraction and on $|V_{td}/V_{ts}|$) result from the present event selection, while the large (small) values are obtained by assuming that for the same selection efficiency as in the present analysis the background is halved. For a luminosity of $\sim 500\ fb^{-1}$ a significant measurement of these modes is expected. The limiting factor for extracting $|V_{td}/V_{ts}|$ is the theoretical uncertainty from $SU(3)$ breaking and the size of the annihilation diagram. The latter uncertainty can be removed by using only $B^0 \to \rho^0\gamma$ events, but for the same significance a factor of four increase in luminosity is required.

Table 2. Extrapolations of the significance, experimental error on the branching fraction and experimental error on $|V_{td}/V_{ts}|$ for the combined $B \to \rho(\omega)\gamma$ modes expected for different luminosities.

Luminosity	significance	$(\sigma_{\mathcal{B}}/\mathcal{B})_{exp}$	$\sigma(V_{td}/V_{ts})$
100 fb^{-1}	1.9 – 2.8 σ	0.38-0.53	0.19-0.27
200 fb^{-1}	2.7 – 3.9 σ	0.28-0.38	0.14-0.19
300 fb^{-1}	3.3 – 4.8 σ	0.23-0.31	0.12-0.15
400 fb^{-1}	3.9 – 5.5 σ	0.20-0.27	0.1-0.14
500 fb^{-1}	4.3 – 6.2 σ	0.18-0.25	0.09-0.13
1000 fb^{-1}	6.0 – 8.7 σ	0.14-0.18	0.07-0.09

4 Outlook

By 2007 *BABAR* expects to record an integrated luminosity of $\sim$ 500 fb^{-1}. This sample will be sufficient to measure the $B \to K^{(*)}\ell^+\ell^-$ and $B \to \rho(\omega)\gamma$ branching fractions with reasonable precision. Due to the theoretical uncertainties, however, tests of the Standard Model will be rather limited. For example, at a luminosity of 1 ab^{-1} the presently quoted theoretical uncertainties for $|V_{td}/V_{ts}|$ will be larger than the extrapolated experimental errors.

Observables that are barely affected by theoretical uncertainties and, therefore, provide excellent tests of the Standard Model are the lepton forward-backward asymmetry as a function of $m_{\ell\ell}$ measured in $B \to K^{(*)}\ell^+\ell^-$ modes and direct *CP* violation in $B \to \rho\gamma$ channels. In SM the lepton forward-backward asymmetry in the B rest frame for dilepton masses below the J/ψ has a characteristic shape, crossing zero at a specific dilepton mass [1]. The zero point is predicted in SM with small uncertainties. With limited statistics we will just determine the zero point, while with high statistics we will be able to measure the entire distribution. Deviations from the SM shape will hint to New Physics. In SM *CP* asymmetries in $B \to \rho\gamma$ could be as large as 12%, but may be modified considerably in models with minimal flavor violation [12]. Precise measurements of the shape of the lepton forward-backward asymmetry and direct *CP* violation in $B \to \rho\gamma$, however, require data samples that are several tens of ab^{-1}.

5 Acknowledgments

I would like to thank the radiative penguin working group for useful discussion and the Norwegian Research Council for support.

References

1. A. Ali *et al.*, Phys. Rev. **D66**, 034002 (2002).
2. P. Colangelo *et al.*, Phys.Rev. **D53**, 3672 (1996), Erratum-ibid. **D57**, 3186 (1998); D. Melikhov *et al.*, Phys.Rev. **D57**, 6814 (1998); C.Q. Geng and C.P. Kao, Phys.Rev. **D54**, 5636 (1996); T.M. Aliev *et al.*, Phys.Lett. **B400**, 194 (1997); A. Ali *et al.*, Phys.Rev. **D61**, 074024 (2000); A. Faessler *et al.*, Eur.Phys.J.direct **C4**,18 (2002); M. Zhong *et al.*, Int.J.Mod.Phys. **A18** 1959 (2003).
3. G.C. Fox and S. Wolfram, Phys. Rev. **Lett. 41**, 1581 (1978).
4. K. Hagiwara *et al.* (Particle Data Group) Phys. Rev. **D66**, 010001 (2002).
5. R.A. Fisher, Ann. Eugenics **7** (1936).
6. B. Aubert *et al.* (*BABAR* collaboration), SLAC-PUB-9323, 33 pp (Jul 2002).
7. T. Skwarnicki, DESY internal report No DESY-F31-86-02 (1986); T. Skwarnicki *et al.* (Crystal Ball collaboration) Phys. Rev Lett. **58**, 972 (1987).
8. H. Albrecht *et al.* (ARGUS collaboration), Phys. Lett. **B241**, 278 (1990).
9. K. Abe *et al.* (BELLE collaboration), Phys. Rev. Lett. **88**, 021801 (2002).
10. B. Aubert *et al.* (*BABAR* collaboration), Phys. Rev **D66**, 032003 (2002).
11. B. Aubert *et al.* (*BABAR* collaboration), SLAC-PUB-9319, 17 pp (Jul 2002).
12. A. Ali and A. Y. Parkhamenko, Eur. Phys. J. C23, 89 (2001).
13. S.W. Bosch and G. Buchalla, Nucl. Phys. **B621**, 459 (2002).
14. B. Aubert *et al.* (*BABAR* collaboration), Phys. Rev Lett. **88**, 101805 (2002).
15. B. Grinstein and D. Pirjol, Phys. Rev. D 62, 093002 (2000).
16. T.E. Coan *et al.* (CLEO collaboration), Phys.Rev. Lett. **84**, 5283 (2000).
17. Y. Ushiroda *et al.* (BELLE collaboration), contributed to BCP4, Ise-Shima, Japan, hep-ex/0101015 (2001).
18. M. Battaglia *et al.*, hep-ex/0304132 (2003).